



CHAOS IN SPATIALLY EXTENDED SYSTEMS VIA THE PEAK-CROSSING BIFURCATION

ARNO BERGER

*Department of Mathematics and Statistics,
University of Canterbury, Christchurch, New Zealand
arno.berger@canterbury.ac.nz*

LEONID A. BUNIMOVICH*

*School of Mathematics, Georgia Institute of Technology,
Atlanta, GA 30332-0160, USA
bunimovh@math.gatech.edu*

Received December 1, 2004; Revised January 22, 2005

Individual sites in spatially extended systems of coupled identical maps may exhibit chaotic behavior even if their intrinsic (local) dynamics is regular and stable. For this to happen it is imperative that the spatial interactions are sufficiently strong. So far, this scenario of generating chaos from simple local dynamics has been established rigorously only for special, very narrow classes of local maps. The present article largely extends previous results by showing that the corresponding mechanism of *peak-crossing* is in fact very general and robust: whenever the local map is sufficiently expanding and exhibits a horseshoe then the emergence of spatial intermittency will be observed in the form of chaotically oscillating sites surrounded by quasi-regular clusters. The results firmly establish peak-crossing as a natural scenario on the route to spacetime chaos.

Keywords: Coupled map lattices; lattice dynamical systems; expanding map.

1. Introduction

Time evolution of spatially extended dynamical systems proceeds by a combination of local dynamics and spatial interactions between local (point) systems. When compared with the dynamics of point (nonextended) systems, the dynamics of extended systems is presently only poorly understood. This imbalance appears to be a major reason why some of the most successful concepts so far in the theory of lattice dynamical systems (anti-integrable limit [MacKay & Aubry, 1994; Aubry, 1997], spacetime chaos [Bunimovich & Sinai, 1988]) deal with small perturbations of spatially extended but non-interacting systems. The fundamental common goal

in these studies is to show (or provide conditions guaranteeing) that the dynamics of the spatially extended system with weak interactions is qualitatively similar to the dynamics with no interactions at all. Under a slightly broader perspective, however, it is a key question in which ways the evolution of spatially extended dynamical systems can differ from the evolution of a collection of noninteracting local systems. In other words, it is most fundamental to understand how spatial interactions qualitatively influence and change the dynamics of extended systems. In a sense, one is thus confronted with bifurcation problems, with the strength of spatial interactions playing the role of a natural bifurcation parameter. Finding generic bifurcations is

*Author for correspondence.

definitely one of the major problems in the theory of spatially extended systems. Some of these bifurcations can naturally be considered as routes to spatial or spatio-temporal chaos. There are at least three generally accepted routes to (temporal) chaos in nonextended systems. It seems natural to expect that there are yet many routes more in spatially extended systems. In this case, however, hardly anything seems to be known at present.

It has been shown in [Bunimovich & Venkatagiri, 1996, 1997] that one scenario for the emergence of spatio-temporal chaos is provided by the so-called *peak-crossing bifurcation*. However, these papers only deal with very narrow, somewhat artificial classes of local maps. Consequently it has been unclear whether this bifurcation might not actually be much more general and robust. In the present paper we show that this is indeed the case: the peak-crossing bifurcation is a very general and robust phenomenon, and it leads to the emergence of spatial intermittency where the sites with chaotic dynamics are surrounded by clusters showing a quasi-regular behavior. This scenario, therefore, should be observable in many extended dynamical systems when the strength of spatial interactions exceeds some (positive) threshold. The present work should be seen as a natural continuation and complement to [Bunimovich & Venkatagiri, 1996, 1997].

This article is organized as follows. In Sec. 2 we provide the necessary definitions for spatially extended systems, and we introduce two simple families of maps which serve as models for more general local maps. Based on these model maps we then formulate our main results and explain their significance. Section 3 contains the proof of these results, broken down into a number of natural steps. In a final section we comment on various interesting questions which arise naturally from the present work and which we think are of considerable importance on the way towards a deeper understanding of spacetime chaos.

2. Definitions and Main Results

We begin by recalling some basic notions for lattice dynamical systems, and we then introduce two one-dimensional model maps which turn out to be helpful in formulating our main results about the peak-crossing bifurcation.

As usual, the sets of positive, non-negative, and all integers are symbolized by \mathbb{N} , \mathbb{N}_0 , \mathbb{Z} , respectively;

also \mathbb{R} stands for the real numbers, and $[a, b]$ is the compact interval with real endpoints $a < b$. Let T, S denote two maps of the unit interval into itself; furthermore let $X := [0, 1]^{\mathbb{Z}^d}$. The space X will serve as the phase space of a spatially extended dynamical system. We denote points $x \in X$ as $x = (x_i)_{i \in \mathbb{Z}^d}$; for $i, j \in \mathbb{Z}^d$ we let $\|i - j\| := \sum_{k=1}^d |i_k - j_k|$. (The choice of this particular norm is motivated solely by keeping all formulae simple.) Generally, a lattice dynamical system is generated by any map $\Phi : X \rightarrow X$ [Kaneko, 1993; Bunimovich, 1995; Chaté & Courbage, 1997]. In this paper, we will exclusively deal with diffusive nearest-neighbor interactions. Our results, however, largely generalize to wider classes of lattice dynamical systems, and we shall occasionally comment on the latter. For a diffusive nearest-neighbor interaction Φ takes the form

$$(\Phi x)_i = T(x_i) + \frac{\varepsilon}{2d} \sum_{j: \|j-i\|=1} (S(x_j) - S(x_i)), \quad \forall i \in \mathbb{Z}^d, \quad (1)$$

where $\varepsilon \geq 0$ quantifies the strength of the interaction between neighboring sites. The special case $T = S$ is usually referred to as a *coupled map lattice* (CML); in this case (1) can be rewritten as

$$(\Phi x)_i = (1 - \varepsilon)T(x_i) + \frac{\varepsilon}{2d} \sum_{j: \|j-i\|=1} T(x_j), \quad \forall i \in \mathbb{Z}^d, \quad (2)$$

which obviously factors as $\Phi = \mathcal{E} \circ \mathcal{T}$ where $\mathcal{T}, \mathcal{E} : X \rightarrow X$ with

$$(\mathcal{T}x)_i = T(x_i),$$

$$(\mathcal{E}x)_i = (1 - \varepsilon)x_i + \frac{\varepsilon}{2d} \sum_{j: \|j-i\|=1} x_j, \quad \forall i \in \mathbb{Z}^d,$$

represent the local (uncoupled) evolution and the global interaction operator, respectively. Thus for CML evolution and interaction act *consecutively*. Another traditional specialization of (1) is $S = id_{[0,1]}$ in which case

$$(\Phi x)_i = T(x_i) + \frac{\varepsilon}{2d} \sum_{j: \|j-i\|=1} (x_j - x_i)$$

$$= T(x_i) - \varepsilon x_i + \frac{\varepsilon}{2d} \sum_{j: \|j-i\|=1} x_j, \quad \forall i \in \mathbb{Z}^d; \quad (3)$$

unless explicitly stated otherwise throughout this paper we will always refer to (3) when using the

term *lattice dynamical system* (LDS). For an LDS according to (3) — and also in the more general situation of (1) with $T \neq S$ — there is no obvious factorization of Φ into (local) evolution and (global) interaction operators; the two fundamental processes of evolution and interaction occur *simultaneously*. Correspondingly, LDS are often used as discretized models of reaction–diffusion equations [Kaneko, 1993; Bunimovich, 1995; Afraimovich & Fernandez, 2000].

We now introduce two families of maps on the unit interval which will serve as models for studying the mechanism of peak-crossing. Typical representatives of both families are depicted in Fig. 1.

The map $L = L_{a,b,c}$, depending on three parameters a, b, c with

$$0 < a < b < \frac{1}{2} < \frac{3}{4} < c < 1, \tag{4}$$

is piecewise linear and tent-like between $1/2$ and 1 ; more specifically,

$$L_{a,b,c}(x) = \begin{cases} a + 2(b - a)x & \text{if } x \in \left[0, \frac{1}{2}\right], \\ c - (c - b)|4x - 3| & \text{if } x \in \left[\frac{1}{2}, 1\right]. \end{cases} \tag{5}$$

The C^1 map $Q = Q_{a,b,c}$ should be thought of as a smooth version of $L_{a,b,c}$. We assume that Q is convex on $[0, 1/2]$ with

$$0 < Q(0) = a < b = Q\left(\frac{1}{2}\right) < \frac{1}{2},$$

and that on $[1/2, 1]$ Q is given by a logistic parabola, i.e.

$$Q_{a,b,c}(x) = b + c(2x - 1)(1 - x), \quad \forall x \in \left[\frac{1}{2}, 1\right],$$

with $c > 0$ and $(3/4) < b + (c/8) < 1$. The characteristic dynamical feature of L and Q (for sufficiently large c) is the existence of a stable attracting fixed point $x^* \in [0, 1/2]$; under iteration of the local map L, Q Lebesgue almost every point is attracted towards x^* .

Piecewise linear maps similar to (yet more contrived than) $L_{a,b,c}$ have been studied in [Bunimovich & Venkatagiri, 1996, 1997] in view of peak-crossing and the emergence of space intermittency for CML and LDS. As explained earlier, the main goal of the present work is to demonstrate that despite their very special (or even accidental) appearance the observations made in these articles hold in fact true under quite general circumstances. We are going to prove that, informally speaking, whenever the local maps of a CML or LDS resembles one of the model maps L or Q then space intermittency via the peak-crossing bifurcation will be observed.

To precisely formulate our main results let $C^{\text{Lip}}[0, 1]$ be the Banach space of all Lipschitz continuous functions on the unit interval endowed with the norm

$$\|f\|_{\text{Lip}} := \max_{x \in [0,1]} |f(x)| + \sup_{x \neq y} \frac{|f(x) - f(y)|}{|x - y|}.$$

We denote by \mathcal{M}^{Lip} the closed subset of $C^{\text{Lip}}[0, 1]$ consisting of all maps of the unit interval into itself, i.e.

$$\mathcal{M}^{\text{Lip}} := \{T \in C^{\text{Lip}}[0, 1] : T([0, 1]) \subset [0, 1]\}.$$

Analogously, \mathcal{M}^1 is the set of all C^1 maps of the unit interval into itself. Clearly, \mathcal{M}^1 is a closed subset of \mathcal{M}^{Lip} . Let λ be any probability measure equivalent to Lebesgue measure m^1 on the unit interval, and define $\Lambda := \bigotimes_{i \in \mathbb{Z}^d} \lambda$. For $n \in \mathbb{N}$, the n -fold composition of Φ with itself will be denoted by Φ^n , and $\Phi^0 = id_X$. In studying the dynamics of Φ we will

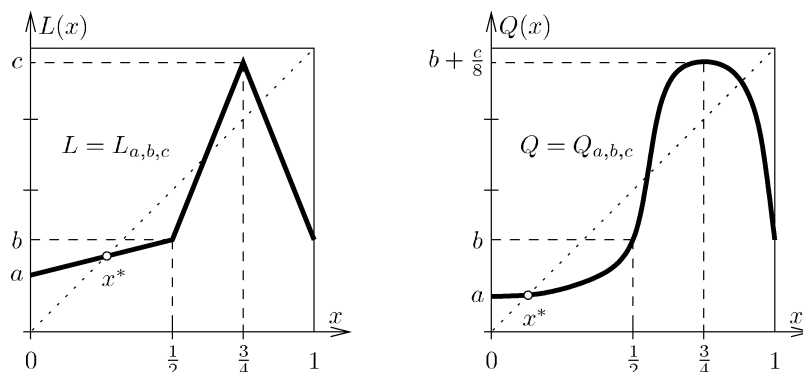


Fig. 1. Two families of model maps: piecewise linear (left) and smooth.

write x_i^n instead of $(\Phi^n x)_i$ for all $n \in \mathbb{N}_0, i \in \mathbb{Z}^d$; in particular, therefore $x_i^0 = x_i$.

Theorem 1. *Let Φ be a CML according to (2) or an LDS according to (3) with Lipschitz continuous local map T . There exists an open set \mathcal{U} in \mathcal{M}^{Lip} , containing L_{a^*,b^*,c^*} for some parameter value (a^*, b^*, c^*) , and an interval $I \subset [1/2, 1]$ as well as numbers $0 < \varepsilon_1 < \varepsilon_2 < \varepsilon_3$ such that for every $T \in \mathcal{U}$ with Λ -probability one there are infinitely many sites $i^* \in \mathbb{Z}^d$ with the following properties:*

- (i) *For every $0 \leq \varepsilon < \varepsilon_1$ and all j with $\|j - i^*\| \leq 2$,*

$$0 \leq x_j^n \leq \frac{1}{2}, \quad \forall n \in \mathbb{N}_0;$$

the dynamics at each site j with $\|j - i^\| \leq 2$ is regular with negative Lyapunov exponent.*

- (ii) *For every $\varepsilon_2 < \varepsilon < \varepsilon_3$,*

$$x_{i^*}^n \in I, \quad \forall n \in \mathbb{N}_0,$$

whereas for all j with $1 \leq \|j - i^\| \leq 2$*

$$0 \leq x_j^n \leq \frac{1}{2}, \quad \forall n \in \mathbb{N}_0;$$

the dynamics at site i^ is chaotic with positive Lyapunov exponent, whereas the sites j with $1 \leq \|j - i^*\| \leq 2$ oscillate regularly in the sense of (i).*

To rephrase the content of Theorem 1 graphically, there are infinitely many “clusters” on the lattice which undergo a transition from “all regular” (Fig. 2, left) to “all-but-one regular and one chaotic” (Fig. 2, right) as the coupling strength ε increases.

One aspect of the local dynamics of $Q_{a,b,c}$ which is well-known to everyone familiar with one-dimensional dynamics is the abundance of (stable)

periodic orbits as c varies. It is a natural question how this abundance of periodic orbits is reflected in CML with local maps resembling $Q_{a,b,c}$.

Theorem 2. *Let Φ be a CML according to (2) with a local map T which is C^1 , and $p \in \mathbb{N}$. There exists an open set $\mathcal{U} \subset \mathcal{M}^1$, containing Q_{a^*,b^*,c^*} for some parameter value (a^*, b^*, c^*) , and disjoint intervals $I_1, \dots, I_p \subset [1/2, 1]$ as well as numbers $0 < \varepsilon_1 < \varepsilon_2 < \varepsilon_3$ such that for every $T \in \mathcal{U}$ with Λ -probability one there are infinitely many sites $i^* \in \mathbb{Z}^d$ with the following properties:*

- (i) *For every $0 \leq \varepsilon < \varepsilon_1$ and all j with $\|j - i^*\| \leq 2$*

$$0 \leq x_j^n \leq \frac{1}{2}, \quad \forall n \in \mathbb{N}_0.$$

- (ii) *For every $\varepsilon_2 < \varepsilon < \varepsilon_3$ and $l = 1, \dots, p$*

$$x_{i^*}^{np+l} \in I_l, \quad \forall n \in \mathbb{N}_0,$$

whereas for all j with $1 \leq \|j - i^\| \leq 2$*

$$0 \leq x_j^n \leq \frac{1}{2}, \quad \forall n \in \mathbb{N}_0.$$

In both cases the motion at each site j with $\|j - i^\| \leq 2$ is regular in the sense of Theorem 1(i).*

It should be noticed that, although the succession of intervals I_l is periodic, the sequence $(x_{i^*}^n)_{n \in \mathbb{N}_0}$ will typically not be periodic. As will be discussed in detail subsequently, the dynamics at each site is genuinely nonautonomous, and strict periodic repetition should therefore not be expected. However, if the sets I_l are small (as they will typically be) then $(x_{i^*}^n)_{n \in \mathbb{N}_0}$ may be thought of as a “noisy” periodic orbit with the noise caused by the motion of the neighboring sites. Under this perspective, the formulation of Theorem 2 appears to be quite natural. Its content could be rephrased

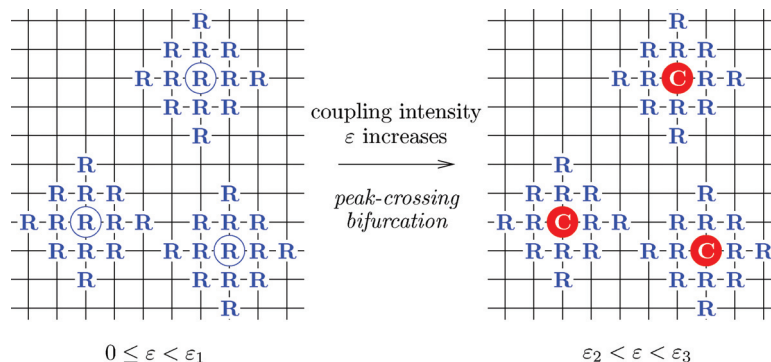


Fig. 2. A visualization of Theorem 1 for $d = 2$. (The letters **R** and **C** symbolise regular and chaotic sites, respectively.)

informally as follows: every *potentially* stable periodic orbit of a map resembling Q_{a^*,b^*,c^*} will become visible at many sites in the spatially extended system through an appropriate (i.e. sufficiently large) coupling; this will happen even though for all practical purposes the corresponding feature is *not* visible in the local map and hence in the so-called anti-integrable limit [Aubry, 1997]. It is for this reason that we advocate peak-crossing as a simple mechanism demonstrating how unstable local complexity and spatial interactions together may generate stable spatio-temporal complexity.

3. Proofs

The proofs of Theorems 1 and 2 can be broken down naturally into a number of steps. In a first step the local dynamics of the maps L and Q is analyzed, and parameters are chosen in such a way that a.e. point shows trivial behavior. Secondly, conditions are imposed on the coupling parameter ε such that peak-crossing can occur while at the same time the regular cluster persists. In a third step it is shown that these conditions are consistent, and an explicit list of parameters is given. Finally, it has to be checked that the overall dynamical picture does not change if the model maps are replaced by a general map T in the respective systems as long as T is sufficiently close to the model map in question. Evidently, the concrete estimates used for the proof depend strongly on whether a CML or an LDS is considered. The structure of the argument, however, is completely identical, as is of course the ultimate statement, i.e. Theorem 1, itself. We therefore present the proof of the CML case in more detail and only hint at the necessary modifications for LDS at the end. Also, once Theorem 1 has been proved completely, the proof of Theorem 2 is largely similar and straightforward.

3.1. Local analysis

The first step towards a proof of Theorem 1 consists of an analysis of the family $L_{a,b,c}$. The local dynamics of $L_{a,b,c}$ is fairly simple: it follows from (4) that $L_{a,b,c}$ has a unique fixed point $x^* \in [0, 1/2]$, and

$$0 < L'_{a,b,c}(x^*) = 2(b - a) < 1,$$

showing that x^* is stable. Furthermore, $L_{a,b,c}$ is expanding on $[1/2, 1]$. To ensure trivial local dynamics, i.e. $\lim_{n \rightarrow \infty} L_{a,b,c}^n(x) = x^*$ for a.e. x , we make use of the following simple fact [Bunimovich & Venkatagiri, 1996].

Proposition 3. For the map $R : \mathbb{R} \rightarrow \mathbb{R}$ defined as

$$R(x) = \begin{cases} \alpha - \gamma_1(\beta - x) & \text{if } x \leq \beta, \\ \alpha - \gamma_2(x - \beta) & \text{if } x > \beta, \end{cases}$$

with $\alpha > \beta$ and $\gamma_1, \gamma_2 > 0$ the following properties are equivalent:

- (i) $\lim_{n \rightarrow \infty} |R^n(x_0)| = \infty$ holds for every $x_0 \in \mathbb{R} \setminus C$ where C is a nowhere dense set of Lebesgue measure zero;
- (ii) $\gamma_1\gamma_2 > \gamma_1 + \gamma_2$.

From Proposition 3 and (5) we deduce that triviality of the local dynamics is ensured if $4(c - b) > 2$. Thus if (4) is augmented by

$$\max\left\{\frac{3}{4}, b + \frac{1}{2}\right\} < c < 1, \tag{6}$$

then, for $\varepsilon = 0$, every individual site i typically evolves in a completely regular way.

3.2. Peak-crossing and persistence of clusters

Assume that $x_j^n \in [0, 1/2]$ for all j with $1 \leq \|j - i^*\| \leq 2$. Since each site has $2d$ neighbors and

$$x_j^{n+1} = (1 - \varepsilon)L(x_j^n) + \frac{\varepsilon}{2d} \sum_{k: \|k-j\|=1} L(x_k^n), \tag{7}$$

we have as an immediate, rough estimate

$$\varepsilon a \leq x_j^{n+1} - (1 - \varepsilon)L(x_j^n) \leq \varepsilon c.$$

To ensure that indeed $x_j^{n+1} \in [0, 1/2]$ we therefore require that $(1 - \varepsilon)b + \varepsilon c < 1/2$ which yields the upper bound

$$\varepsilon < 1 - \frac{2c - 1}{2(c - b)}. \tag{8}$$

To analyze the dynamics at site i^* we introduce the maps

$$L_\varepsilon^\pm(x) := (1 - \varepsilon)L(x) + \varepsilon \frac{b + a}{2} \pm \varepsilon \frac{b - a}{2}, \quad \forall x \in [0, 1].$$

(Here and in the sequel, relations containing \pm or \mp should be read as two independent equations containing exclusively the upper and lower signs, respectively.) Clearly $L_\varepsilon^+(x_{i^*}^n) \geq x_{i^*}^{n+1} \geq L_\varepsilon^-(x_{i^*}^n)$. For stationary, i.e. nontransient, chaotic dynamics to occur at site i^* we require that $|L_\varepsilon^\pm| = 4(1 - \varepsilon)(c - b) > 1$ and $L_\varepsilon^-(3/4) > 3/4$. This leads

to the two conditions

$$\varepsilon < 1 - \frac{1}{4(c-b)} \quad \text{and} \quad \varepsilon < \frac{c - \frac{3}{4}}{c - a}, \tag{9}$$

respectively. More importantly, however, we require that orbits at site i^* can get “trapped” in the right half of the interval, i.e. for all $x_{i^*}^0$ from an interval of positive length we have $x_{i^*}^n \in [1/2, 1]$ for all n . To this end let x_ε^\pm denote the unique fixed point of L_ε^\pm in $[1/2, 3/4]$, and define y_ε^\pm as the (also unique) point in $[3/4, 1]$ with $L_\varepsilon^\pm(y_\varepsilon^\pm) = x_\varepsilon^\pm$. The trapping condition then reads (see also Fig. 3)

$$L_\varepsilon^+ \left(\frac{3}{4} \right) < y_\varepsilon^-. \tag{10}$$

A lengthy yet elementary calculation shows that (10) is equivalent to

$$\varphi(u) := \left(u - \frac{1}{2} \right) \left(u - \frac{3}{4} + b \right) < -\frac{1}{4}\varepsilon(b-a), \tag{11}$$

where $u := (1 - \varepsilon)(c - b)$. Evidently, (11) will give rise to a lower and an upper bound for ε . These

bounds, however, are not easily extracted from (11). We therefore aim at strengthening and thereby simplifying this latter condition. To do so we will henceforth assume that the parameters a, b, c satisfy

$$a > \frac{3}{8} \quad \text{and} \quad c > \max \left\{ b + \frac{1}{2}, \frac{9}{8} - \frac{b}{2} \right\}. \tag{12}$$

Furthermore, we replace the parabola defined by φ on the left-hand side of (11) by a wedge-shaped, piecewise linear function ψ with the same zeros and apex (see Fig. 4),

$$\psi(u) = \frac{4b-1}{64}(1-4b+|8u-5+4b|).$$

Observe that $\varphi(u) \leq \psi(u) \leq 0$ for all $u \in [3/4 - b, 1/2]$. Also, note that (8) is equivalent to $u > c - (1/2)$. It will become clear shortly that under the conditions of (12) it is the inequality (8) which yields the tightest upper bound on ε . To obtain a nonempty interval for ε for which trapping actually occurs we therefore require that

$$\psi \left(c - \frac{1}{2} \right) < -\frac{1}{4}\varepsilon(b-a),$$

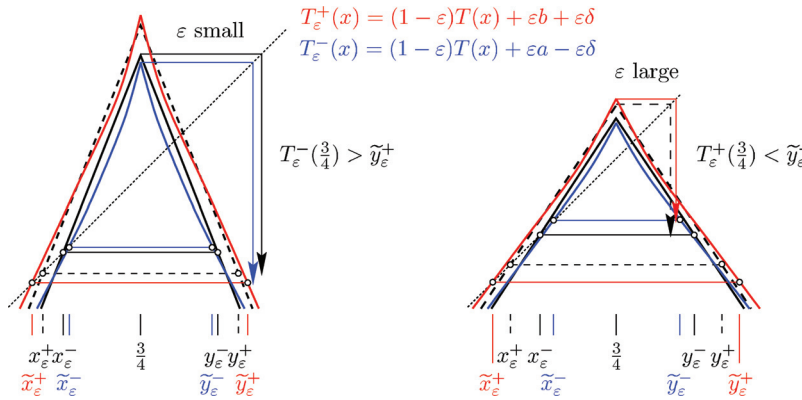


Fig. 3. Visualizing nontrapping for small ε (left) and trapping for larger ε in the CML case; the situation is analogous for LDS. (The piecewise linear maps L_ε^\pm are indicated by a dashed and solid black line, respectively; general maps T_ε^\pm , indicated by colored graphs, are dealt with in Sec. 3.4.)

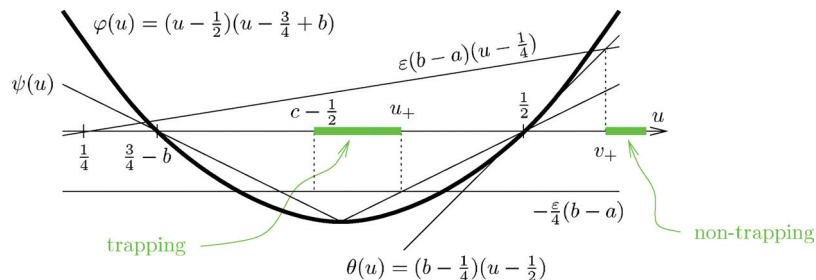


Fig. 4. Simplifying the trapping and nontrapping conditions (11) and (22), respectively.

which is readily seen to be equivalent to

$$\varepsilon < \frac{4b - 1}{2(b - a)}(1 - c). \tag{13}$$

3.3. Consistency of conditions

We first collect all the conditions on ε encountered so far: combining (8), (9) and (13) we have

$$\varepsilon < \min \left\{ 1 - \frac{2c - 1}{2(c - b)}, 1 - \frac{1}{4(c - b)}, \frac{c - \frac{3}{4}}{c - a}, \frac{4b - 1}{2(b - a)}(1 - c) \right\}. \tag{14}$$

It is easy to check that the minimum in (14) is in fact attained with the first term provided that

$$c < 1 - 4(b - a)(1 - 2b). \tag{15}$$

For (15) to be consistent with the second condition in (12) it is necessary that $b - a < 1/16$. An updated list of restrictions on the parameters a, b, c therefore reads as follows:

$$\begin{aligned} \frac{3}{8} < a < \frac{1}{2}, \\ a < b < \min \left\{ \frac{1}{2}, a + \frac{1}{16} \right\}, \\ \max \left\{ b + \frac{1}{2}, \frac{9}{8} - \frac{b}{2} \right\} < c < 1 - 4(b - a)(1 - 2b). \end{aligned} \tag{16}$$

We shall always assume (16) in the sequel. The trapping condition (10) will be satisfied if $c - 1/2 < u_+$ or, equivalently, if

$$1 - \frac{u_+}{c - b} < \varepsilon < 1 - \frac{2c - 1}{2(c - b)} =: \hat{\varepsilon}_3; \tag{17}$$

here the quantity u_+ is found from the condition $\psi(u_+) = -(1/4)\varepsilon(b - a)$ together with $u_+ > 5/8 - b/2$ (see Fig. 4) as

$$u_+ = \frac{1}{2} - 2\varepsilon \frac{b - a}{4b - 1}. \tag{18}$$

It is straightforward to check that with this the left-hand inequality in (17) turns into

$$\varepsilon > \left(1 - 2 \frac{b - a}{(4b - 1)(c - b)} \right)^{-1} \left(1 - \frac{1}{2(c - b)} \right). \tag{19}$$

For practical purposes we replace (19) by the slightly stricter condition

$$\varepsilon > (1 - 8(b - a))^{-1} \left(1 - \frac{1}{2(c - b)} \right) =: \hat{\varepsilon}_2, \tag{20}$$

which — it turns out — is still consistent with the right inequality in (17), that is, $\hat{\varepsilon}_2 < \hat{\varepsilon}_3$.

Recall that for $\varepsilon = 0$ the local dynamics is trivial, i.e. the orbit of a.e. point $x \in [0, 1]$ does not get trapped but rather converges to the stable fixed point x^* . Nontrapping persists for positive ε as long as the condition

$$L_\varepsilon^-\left(\frac{3}{4}\right) > y_\varepsilon^+ \tag{21}$$

is met (see Fig. 3). Again, (21) can be reformulated equivalently as

$$\varphi(u) = \left(u - \frac{1}{2}\right) \left(u - \frac{3}{4} + b\right) > \varepsilon(b - a) \left(u - \frac{1}{4}\right), \tag{22}$$

where $u = (1 - \varepsilon)(c - b)$ as before. As was the case with the trapping condition (11), relation (22) does not seem to directly yield any manageable positive upper bound on ε . We therefore again replace the parabola given by φ by a simpler object, this time its tangent at $u = 1/2$ described by the linear function

$$\theta(u) = \left(b - \frac{1}{4}\right) \left(u - \frac{1}{2}\right);$$

the corresponding bound v_+ (see Fig. 4) can be found easily from $\theta(v_+) = \varepsilon(b - a)(v_+ - 1/4)$. Still it is convenient to simplify the resulting formula. Assuming

$$b - a < \frac{1}{20}, \tag{23}$$

we deduce that $\hat{\varepsilon}_2 < 1/3$. Since for nontrapping clearly we are interested in the case $\varepsilon < \hat{\varepsilon}_2$, the explicit formula for v_+ can be simplified to $v_+ > 7/13$ and therefore

$$\varepsilon < 1 - \frac{7}{13(c - b)} =: \hat{\varepsilon}_1. \tag{24}$$

For $\hat{\varepsilon}_1$ to be positive we must have $c > b + 7/13$ which in turn is consistent with the last condition in (16) provided that $b < 3/7$.

We summarize our results in the following list of relations between the parameters of the local map

$L_{a,b,c}$:

$$\frac{3}{8} < a < \frac{3}{7},$$

$$a < b < \min\left\{\frac{3}{7}, a + \frac{1}{20}\right\},$$

$$\max\left\{b + \frac{7}{13}, \frac{9}{8} - \frac{1}{2}b\right\} < c < 1 - 4(b - a)(1 - 2b). \tag{25}$$

If a, b, c satisfy (25) then for $0 \leq \varepsilon < \hat{\varepsilon}_1$ the dynamics is regular at each site j with $\|j - i^*\| \leq 2$. On the other hand, for $\hat{\varepsilon}_2 < \varepsilon < \hat{\varepsilon}_3$ at site i^* every orbit starting in the interval $[x_\varepsilon^-, y_\varepsilon^-]$ will stay there forever (it is getting “trapped”), and the dynamics in this interval is more irregular in the sense that, due to the expansiveness of L_ε^\pm , nearby trajectories diverge exponentially. We shall make this statement more precise towards the end of Sec. 3.5.

3.4. General local maps

We are now going to demonstrate that the peak-crossing scenario observed in the preceding section for $L_{a,b,c}$ with appropriate parameter values can be found for $T \in \mathcal{M}^{\text{Lip}}$ as well, provided that T is sufficiently close to $L_{a,b,c}$, that is for $\|T - L_{a,b,c}\|_{\text{Lip}} < \delta$ with some sufficiently small δ . The estimates in this section will automatically yield an explicit upper bound for δ .

We first fix parameter values a^*, b^*, c^* which satisfy (25); by means of the corresponding quantities $\hat{\varepsilon}_1, \hat{\varepsilon}_2, \hat{\varepsilon}_3$ we introduce for further use

$$\varepsilon_1 := \hat{\varepsilon}_1, \quad \varepsilon_2 := \frac{2\hat{\varepsilon}_2 + \hat{\varepsilon}_3}{3}, \quad \varepsilon_3 := \frac{\hat{\varepsilon}_2 + 2\hat{\varepsilon}_3}{3}.$$

Assume now that $\|T - L_{a^*,b^*,c^*}\|_{\text{Lip}} < \delta$. At sites j with $1 \leq \|j - i^*\| \leq 2$ we see from (7) with L replaced by T that

$$\varepsilon(a - \delta) \leq x_j^{n+1} - (1 - \varepsilon)T(x_j^n) \leq \varepsilon(c + \delta). \tag{26}$$

Thus, for the cluster to persist, i.e. $x_j^{n+1} \in [0, 1/2]$, we impose the condition

$$(1 - \varepsilon)(b + \delta) + \varepsilon(c + \delta) < \frac{1}{2}, \tag{27}$$

which gives an upper bound for δ ,

$$\delta < \frac{1}{2} - b - \varepsilon(c - b) = (c - b)(\hat{\varepsilon}_3 - \varepsilon). \tag{28}$$

Since we will be interested only in the case $\varepsilon \leq \varepsilon_3$ we define

$$\hat{\delta}_1 := (c - b)(\hat{\varepsilon}_3 - \varepsilon_3) = \frac{1}{3}(c - b)(\hat{\varepsilon}_3 - \hat{\varepsilon}_2), \tag{29}$$

so that for $\delta < \hat{\delta}_1$ the regular cluster around i^* persists. To deal with the site i^* itself, in view of (26) we define

$$T_\varepsilon^\pm(x) := (1 - \varepsilon)T(x) + \varepsilon\frac{b+a}{2} \pm \varepsilon\frac{b-a}{2} \pm \varepsilon\delta;$$

then clearly $T_\varepsilon^-(x_{i^*}^n) \leq x_{i^*}^{n+1} \leq T_\varepsilon^+(x_{i^*}^n)$. As in Sec. 3.2 we require that T_ε^\pm are expansive, i.e. $(1 - \varepsilon)(4(c - b) - \delta) > 1$, and also that $T_\varepsilon^-(3/4) > 3/4$. Taking into account that $a > 1/8, c - b > 7/13$ and $\varepsilon < \hat{\varepsilon}_3$, these two conditions can be simplified to

$$\delta < \frac{14}{39}(c - b)(\hat{\varepsilon}_3 - \hat{\varepsilon}_2) \quad \text{and} \tag{30}$$

$$\delta < \frac{1}{3}(c - a)(\hat{\varepsilon}_3 - \hat{\varepsilon}_2),$$

respectively. Since $b > a$, both inequalities in (30) are obviously implied by $\delta < \hat{\delta}_1$. To correctly write down the trapping condition for T let $\tilde{x}_\varepsilon^\pm$ denote the (unique) fixed point of T_ε^\pm in $[1/2, 3/4]$; as in Sec. 3.2 let $\tilde{y}_\varepsilon^\pm$ be the unique point in $[3/4, 1]$ with $T_\varepsilon(\tilde{y}_\varepsilon^\pm) = \tilde{x}_\varepsilon^\pm$ (see Fig. 3). From the estimate

$$\begin{aligned} T_\varepsilon^\pm(x) &\leq (1 - \varepsilon)(L(x) + \delta) + \varepsilon\frac{a+b}{2} \pm \varepsilon\frac{b-a}{2} + \varepsilon\delta \\ &= L_\varepsilon^\pm(x) + \delta = x_\varepsilon^\pm \\ &\quad + 4(1 - \varepsilon)(c - b)(x - x_\varepsilon^\pm) + \delta \\ &= x + (4(1 - \varepsilon)(c - b) - 1)(x - x_\varepsilon^\pm) + \delta, \end{aligned}$$

we deduce that $\tilde{x}_\varepsilon^\pm - x_\varepsilon^\pm \geq -\delta(4(1 - \varepsilon)(c - b) - 1)^{-1}$; from the reverse inequality with δ replaced by $-\delta$ we therefore obtain

$$|\tilde{x}_\varepsilon^\pm - x_\varepsilon^\pm| < \frac{\delta}{4(1 - \varepsilon)(c - b) - 1}. \tag{31}$$

It is straightforward to see that (31) also holds with x replaced by y . The trapping condition now reads $T_\varepsilon^+(3/4) < \tilde{y}_\varepsilon^-$ or, slightly stronger,

$$(1 - \varepsilon)c + \varepsilon b + \delta < y_\varepsilon^- - \frac{\delta}{4(1 - \varepsilon)(c - b) - 1}. \tag{32}$$

Similarly to (11) this condition can be formulated equivalently as

$$\left(u - \frac{1}{2}\right)\left(u - \frac{3}{4} + b\right) + \frac{1}{4}\varepsilon(b - a) < -\delta u, \tag{33}$$

and it of course reduces to the former condition for $\delta = 0$. Since for trapping $u < u_+ < 1/2$ (recall (18) and Fig. 3), condition (33) can be replaced by

$$\delta < 2\left(\frac{1}{2} - u_+\right)\left(u_+ - \frac{3}{4} + b\right) - \frac{1}{2}\varepsilon(b - a),$$

which, after taking into account (18) and $\hat{\varepsilon}_2 < \varepsilon < \hat{\varepsilon}_3$, leads to

$$\delta < \hat{\varepsilon}_2(b - a) \left(\frac{1}{2} - 8\hat{\varepsilon}_3 \frac{b - a}{(4b - 1)^2} \right) =: \hat{\delta}_2; \quad (34)$$

it is readily confirmed that $\hat{\delta}_2 > 0$. To see the mechanism of peak-crossing in place for T we must ensure that trapping does *not* occur for ε sufficiently close to zero. The relevant condition, corresponding to (21), is that $T_\varepsilon^-(3/4) > \tilde{y}_\varepsilon^+$ or, again slightly stricter,

$$(1 - \varepsilon)c + \varepsilon a - \delta > y_\varepsilon^+ + \frac{\delta}{4(1 - \varepsilon)(c - b) - 1}. \quad (35)$$

This can be seen to be equivalent to

$$\left(u - \frac{1}{2}\right) \left(u - \frac{3}{4} + b\right) - \varepsilon(b - a) \left(u - \frac{1}{4}\right) > \delta u, \quad (36)$$

which corresponds to (22) and reduces to the latter for $\delta = 0$. Since clearly $v_+ \leq u \leq c - b$, the inequality (36) will be satisfied if only $(c - b)\delta < (v_+ - 1/2)^2$. As discussed in the argument leading to (24) $v_+ > 7/13$. This in turn yields the bound

$$\delta < \frac{1}{(26)^2(c - b)} =: \hat{\delta}_3. \quad (37)$$

Finally, it has to be checked that the local dynamics of T with $\|T - L_{a^*, b^*, c^*}\|_{\text{Lip}} < \delta$ is essentially the same as the local dynamics of L_{a^*, b^*, c^*} . For T to have a unique stable fixed point in $[0, 1/2]$ we require that

$$\delta < a, \quad \delta < \frac{1}{2} - b \quad \text{and} \quad \delta < 2(b - a). \quad (38)$$

The conditions that T be expansive and $T(3/4) > 3/4$ lead to

$$\delta < 4(c - b) - 1 \quad \text{and} \quad \delta < c - \frac{3}{4}, \quad (39)$$

respectively. The nontrapping condition now simply reads $c - \delta > y_0 + \delta(4(c - b) - 1)^{-1}$ which gives

$$\delta < \left(c - \frac{3}{4}\right) \left(1 - \frac{1}{2(c - b)}\right). \quad (40)$$

The bounds (38)–(40) are less restrictive than (28), (34) and (37). This is obvious intuitively as, for instance, the nontrapping condition $T_\varepsilon^-(3/4) > \tilde{y}_\varepsilon^+$ becomes more restrictive as ε increases; it can, however, also be confirmed directly by means of a straightforward yet lengthy manipulation of the inequalities involved.

As a result of this section we have proved that with a^*, b^*, c^* chosen according to (25) and with $\|T - L_{a^*, b^*, c^*}\|_{\text{Lip}} < \delta$ where

$$\delta < \min\{\hat{\delta}_1, \hat{\delta}_2, \hat{\delta}_3\} =: \hat{\delta}, \quad (41)$$

the CML with local map T has trivial dynamics at all sites j for $\|j - i^*\| \leq 2$ for $0 \leq \varepsilon < \varepsilon_1$, whereas peak-crossing occurs for $\varepsilon_2 < \varepsilon < \varepsilon_3$. To give a specific example, an admissible choice of parameters would be

$$a^* = 0.4, \quad b^* = 0.42, \quad c^* = 0.97,$$

which in turn yields

$$\varepsilon_1 = 0.0210, \quad \varepsilon_2 = 0.1206, \quad \varepsilon_3 = 0.1330, \quad (42)$$

as well as

$$\hat{\delta} = 9.7331 \cdot 10^{-4}.$$

3.5. Conclusion of the proof of Theorem 1

Given the preparations in previous sections the completion of Theorem 1 is now fairly simple. Recall the definition of the points $x_\varepsilon^-, y_\varepsilon^-$ (see Fig. 3) and let $J_\varepsilon := [x_\varepsilon^-, y_\varepsilon^-]$. A short calculation yields

$$\begin{aligned} \lambda^1(J_\varepsilon) &= 2 \frac{c - \frac{3}{4} - \varepsilon(c - a)}{4(c - b)(1 - \varepsilon) - 1} \\ &= \frac{c - a}{2(c - b)} \cdot \frac{\frac{c - \frac{3}{4}}{c - a} - \varepsilon}{1 - \frac{1}{4(c - b)} - \varepsilon} \end{aligned}$$

which decreases with increasing ε . Define I_0 to be the interval

$$I_0 := \left[x_{\varepsilon_3}^- + \frac{\delta}{4(c - b)(1 - \varepsilon_3) - 1}, y_{\varepsilon_3}^- - \frac{\delta}{4(c - b)(1 - \varepsilon_3) - 1} \right]; \quad (43)$$

then clearly $[\tilde{x}_\varepsilon^-, \tilde{y}_\varepsilon^-] \supset I_0$ for all $0 \leq \varepsilon \leq \varepsilon_3$, and

$$\begin{aligned} m^1(I_0) &= 2 \frac{c - \frac{3}{4} - \varepsilon_3(c - a) - \delta}{4(c - b)(1 - \varepsilon_3) - 1} \\ &> \frac{1}{2} \left(1 - \hat{\varepsilon}_3 \frac{c - a}{c - \frac{3}{4}} \right) > 0. \end{aligned}$$

On the other hand, it is easily checked that $[\tilde{x}_\varepsilon^-, \tilde{y}_\varepsilon^-] \subset I$ for all $0 \leq \varepsilon \leq \varepsilon_3$ where

$$I := \left[x_0 - \frac{\hat{\delta}}{4(c-b)-1}, y_0 + \frac{\hat{\delta}}{4(c-b)-1} \right]. \quad (44)$$

Inserting the estimates for all the quantities involved, it is possible to derive the (very rough) estimate $m^1(I) < 46/105 < 1/2$.

Suppose now that for some $i^* \in \mathbb{Z}^d$ we have $x_{i^*}^0 \in I_0$ and $0 \leq x_j^0 \leq 1/2$ for all j with $1 \leq \|j - i^*\| \leq 2$. As the quintessence of our efforts above we know that whenever the local map T of a CML satisfies $\|T - L_{a^*, b^*, c^*}\|_{\text{Lip}} < \hat{\delta}$ we have for $0 \leq \varepsilon < \varepsilon_1$ that

$$0 \leq x_{i^*}^n \leq \frac{1}{2} \quad \text{and} \quad 0 \leq x_j^n \leq \frac{1}{2} \quad \forall n \in \mathbb{N},$$

whereas for $\varepsilon_2 < \varepsilon < \varepsilon_3$

$$x_{i^*}^n \in I \quad \text{and} \quad 0 \leq x_j^n \leq \frac{1}{2} \quad \forall n \in \mathbb{N}.$$

Thus the peak-crossing bifurcation occurs for T .

To clarify the dynamics at individual sites notice first that T is differentiable almost everywhere, as are therefore the induced maps T_ε^\pm . At each site i we have $x_i^{n+1} = (1 - \varepsilon)T(x_i^n) + a_n$ where the numbers a_n depend, generally speaking, on the history up to step n of all sites j with $\|j - i\| \leq n$. The Lyapunov exponent of any trajectory $(x_i^n)_{n \in \mathbb{N}_0}$ is

$$\begin{aligned} \overline{\lim}_{n \rightarrow \infty} \frac{1}{n} \log \left| \frac{d}{dx_i^0} x_i^n \right| &= \overline{\lim}_{n \rightarrow \infty} \frac{1}{n} \log \left| \prod_{l=1}^n \frac{dx_i^l}{dx_i^{l-1}} \right| \\ &= \overline{\lim}_{n \rightarrow \infty} \frac{1}{n} \sum_{l=1}^n \log |(1 - \varepsilon)T'(x_i^{l-1})|, \end{aligned}$$

which is well-defined almost everywhere. For $\varepsilon_2 < \varepsilon < \varepsilon_3$ and $\|T - L_{a^*, b^*, c^*}\|_{\text{Lip}} < \hat{\delta}$ we have, for a.e. $x \in [1/2, 1]$,

$$\begin{aligned} |(1 - \varepsilon)T'(x)| &> (1 - \hat{\varepsilon}_3)(4(c^* - b^*) - \hat{\delta}) \\ &> \left(c - \frac{1}{2}\right) \left(4 - \frac{1}{3}(\hat{\varepsilon}_3 - \hat{\varepsilon}_2)\right) > 1. \end{aligned}$$

Consequently, if $x_{i^*}^0 \in I_0$ then typically the Lyapunov exponent of $(x_{i^*}^n)_{n \in \mathbb{N}_0}$ is positive, a fact manifesting itself in an erratic motion with exponential divergence of nearby trajectories. On the other hand

$$|(1 - \varepsilon)T'(x)| < 2(b^* - a^*) + \hat{\delta} < 1$$

for almost every $x \in [0, 1/2]$. Therefore, if $1 \leq \|j - i^*\| \leq 2$ and $x_j^0 \in [0, 1/2]$ then the

Lyapunov exponent of $(x_j^n)_{n \in \mathbb{N}_0}$ is negative, resulting in a quasi-regular, nonautonomous motion with rapid convergence of nearby trajectories. For $0 \leq \varepsilon < \varepsilon_1$ the latter is also true at site i^* because eventually almost every orbit finds itself in the left half of the interval $[0, 1]$.

Let now λ be any probability measure on the unit interval equivalent to Lebesgue measure m^1 , and $\Lambda = \bigotimes_{i \in \mathbb{Z}^d} \lambda$. Clearly $\lambda(I_0)\lambda([0, 1/2]) > 0$. Therefore, if the initial value x_i^0 at each site is chosen independently according to λ , that is, if $(x_i^0)_{i \in \mathbb{Z}^d}$ is distributed according to Λ , then with Λ -probability one there are infinitely many sites i^* such that $x_{i^*}^0 \in I_0$ and $x_j^0 \in [0, 1/2]$ for all $1 \leq \|j - i^*\| \leq 2$. For each such cluster and for every map $T \in \mathcal{M}^{\text{Lip}}$ with $\|T - L_{a^*, b^*, c^*}\|_{\text{Lip}} < \hat{\delta}$ therefore a transition from regular to chaotic motion at site i^* occurs as ε increases from $\varepsilon = 0$ to $\varepsilon = \varepsilon_3$. This completes the proof of Theorem 1 for the CML case.

3.6. Necessary modifications for LDS

The proof of Theorem 1 for LDS is overall very similar to the CML case. However, some details deserve extra mentioning. Notice for instance that for $a = b$ the dynamics at site i^* of a CML with local map $L_{a,b,c}$ becomes actually autonomous [Bunimovich & Venkatagiri, 1996]. Consequently, for CML the appearance of a peak-crossing bifurcation may not come as a complete surprise. On the other hand, the local dynamics for an LDS with $\varepsilon > 0$ is always genuinely nonautonomous. As there is no way to completely suppress the influence of the neighboring sites for $\varepsilon > 0$, it is less obvious that peak-crossing can nevertheless occur [Bunimovich & Venkatagiri, 1997]. As will be outlined shortly, to prove Theorem 1 for LDS it is imperative to more carefully analyze the dynamics at the regular sites in the cluster. (Recall that in the CML case the very rough estimate $x_j^n \in [0, 1/2]$ for $1 \leq \|j - i^*\| \leq 2$ was all that was needed; also, a review of the arguments above shows that the size of the clusters could actually have been reduced.) From (3) with $T = L$ it follows that at site i^* of an LDS we have

$$x_{i^*}^{n+1} - (L(x_{i^*}^n) - \varepsilon x_{i^*}^n) = \frac{\varepsilon}{2d} \sum_{j: \|j - i^*\| = 1} x_j^n.$$

In order to not let the contribution on the right-hand side vary too much we must keep control over the actual variation of x_j^n for all the neighboring sites j around i^* . To this end we observe that if $\|j - i^*\| = 1$ then the $2d$ neighbors of the site j

fall into three categories: one neighbor of course is the site i^* while all other $2d - 1$ neighbors k satisfy $\|k - i^*\| = 2$; among the latter, one site has itself only one neighboring site which belongs to the cluster whereas the $2d - 2$ remaining k have two neighbors within the cluster. To locate x_j^n with sufficient accuracy we consider the points $\xi_\varepsilon, \eta_\varepsilon, \zeta_\varepsilon$, defined as the unique solution of

$$L(\xi_\varepsilon) - \varepsilon\xi_\varepsilon + \frac{\varepsilon}{2d}\left(\frac{3}{4} + \eta_\varepsilon + (2d - 2)\zeta_\varepsilon\right) = \xi_\varepsilon,$$

$$L(\eta_\varepsilon) - \varepsilon\eta_\varepsilon + \frac{\varepsilon}{2d}\left(d - \frac{1}{2} + \xi_\varepsilon\right) = \eta_\varepsilon, \quad (45)$$

$$L(\zeta_\varepsilon) - \varepsilon\zeta_\varepsilon + \frac{\varepsilon}{2d}(d - 1 + 2\xi_\varepsilon) = \zeta_\varepsilon,$$

where $0 < \xi_\varepsilon, \eta_\varepsilon, \zeta_\varepsilon < 1/2$. Here ξ_ε should be thought of as a (hopefully good) guess for x_j^n with $\|j - i^*\| = 1$, whereas $\eta_\varepsilon, \zeta_\varepsilon$ are guesses for x_j^n with $\|j - i^*\| = 2$ and j belonging, respectively, to the first and second type of sites described above. Clearly, for $\varepsilon = 0$ we have $\xi_0 = \eta_0 = \zeta_0 = x^*$. Working out exact expressions for $\xi_\varepsilon, \eta_\varepsilon, \zeta_\varepsilon$ is quite cumbersome. Since previous work [Bunimovich & Venkatagiri, 1997] and numerical evidence suggest that admissible values for ε will in any case be rather small, we content ourselves with the first order approximations

$$\xi_\varepsilon = x^* + \frac{1}{8d} \cdot \frac{3(1 - 2b) + 2a}{(1 - 2(b - a))^2} \varepsilon + \mathcal{O}(\varepsilon^2),$$

$$\eta_\varepsilon = x^* + \frac{2d - 1}{4d} \cdot \frac{1 - 2b}{(1 - 2(b - a))^2} \varepsilon + \mathcal{O}(\varepsilon^2),$$

$$\zeta_\varepsilon = x^* + \frac{d - 1}{2d} \cdot \frac{1 - 2b}{(1 - 2(b - a))^2} \varepsilon + \mathcal{O}(\varepsilon^2),$$

which immediately follow from (45). Assuming now that $\varepsilon < 1/10$ and

$$x_{i^*}^n \in \left[\frac{1}{2}, 1\right],$$

$$x_j^n \in \left[\xi_\varepsilon - \frac{1}{6}\varepsilon, \xi_\varepsilon + \frac{1}{6}\varepsilon\right] \quad \forall j \text{ with } \|j - i^*\| = 1,$$

$$x_j^n \in [\eta_\varepsilon - \varepsilon, \eta_\varepsilon + \varepsilon] \quad \forall j \text{ with } \|j - i^*\| = 2 \text{ having one neighbor in the cluster,}$$

$$x_j^n \in [\zeta_\varepsilon - \varepsilon, \zeta_\varepsilon + \varepsilon] \quad \forall j \text{ with } \|j - i^*\| = 2 \text{ having two neighbors in the cluster,} \quad (46)$$

it is straightforward to check that this configuration persists, i.e. (46) holds with n replaced by $n + 1$.

Obviously, (46) provides much more precise information about x_j^n for j from the cluster around i^* than was needed in the CML case.

We now turn towards an analysis of the site i^* . Defining

$$L_\varepsilon^\pm(x) := L(x) - \varepsilon x + \varepsilon\xi_\varepsilon \pm \frac{1}{6}\varepsilon^2,$$

we have $L_\varepsilon^+(x_{i^*}^n) \geq x_{i^*}^{n+1} \geq L_\varepsilon^-(x_{i^*}^n)$. As in the CML case we require that $(L_\varepsilon^\pm)' = 4(c - b) - \varepsilon > 1$ and $L_\varepsilon^-(3/4) > 3/4$, which leads to

$$\varepsilon < 4(c - b) - 1 \quad \text{and} \quad c - \frac{3}{4}\varepsilon > \frac{451}{600}, \quad (47)$$

respectively, where in deriving the second inequality we have used $\xi_\varepsilon > 0$ and $\varepsilon < 1/10$. Again the trapping condition is

$$L_\varepsilon^+\left(\frac{3}{4}\right) < y_\varepsilon^-, \quad (48)$$

where $L_\varepsilon^\pm(y_\varepsilon^\pm) = x_\varepsilon^\pm = L_\varepsilon^\pm(x_\varepsilon^\pm)$ with $1/2 < x_\varepsilon^\pm < 3/4 < y_\varepsilon^\pm < 1$ (see (10) and Fig. 3). As in the CML case condition (48) can be restated in an equivalent yet manageable way. Indeed, a short calculation turns (48) into

$$\left(L_\varepsilon^-\left(\frac{3}{4}\right) - \frac{3}{4}\right)(16v^2 - 8v - \varepsilon^2) + \frac{1}{3}\varepsilon^2(16v^2 - 4 - \varepsilon^2 - \varepsilon) < 0, \quad (49)$$

where $v := c - b$. Since the left-most factor was assumed positive we see that (49) is satisfied for small ε provided that $16v^2 - 8v < \varepsilon^2$, or equivalently

$$\varepsilon > \sqrt{8v(2v - 1)}. \quad (50)$$

Recall from Sec. 3.1 that $v > 1/2$ and $\varepsilon < 4v - 1$; in addition we have assumed $\varepsilon < 1/10$ in the run-up to (46). The reader may wish to check that all these conditions are simultaneously satisfied in the region

$$\left\{(\varepsilon, v) : 0 < \varepsilon < \frac{1}{16}, \frac{1}{2} < v < \frac{1}{4} + \frac{1}{4}\sqrt{1 + \varepsilon^2}\right\}$$

in the (ε, v) -plane. Thus appropriately choosing all parameters will enable the peak-crossing scenario for LDS with local map L . Note, however, that the estimates used are more delicate than in the CML case, and the admissible region in parameter space typically is much narrower. Nevertheless, further analysis is more or less identical with the CML case. We therefore omit the details. A possible list of parameters for which the peak-crossing bifurcation

can be observed with the local map $L = L_{a,b,c}$ is as follows:

$$\begin{aligned} \frac{3}{10} < a < \frac{7}{20}, \\ a < b < \min\left\{\frac{7}{20}, a + \frac{1}{40}\right\}, \\ b + \frac{1}{2} < c < \min\left\{b + \frac{1}{4} + \frac{1}{4}\sqrt{1 + 4(b-a)^2}, \right. \\ \left. \frac{13}{12} - \frac{2}{3}b\right\}. \end{aligned} \tag{51}$$

This set of inequalities is the true analogue of (25); the corresponding thresholds for ε are (with the same meaning as in Sec. 3.4)

$$\begin{aligned} \hat{\varepsilon}_1 &= (4c - 3)\frac{2(c - b) - 1}{6(c - b) - 2}, \\ \hat{\varepsilon}_2 &= \sqrt{8(c - b)(2(c - b) - 1)}, \\ \hat{\varepsilon}_3 &= 4(b - a). \end{aligned}$$

With an appropriate, sufficiently small $\hat{\delta} > 0$ the remainder of the proof of Theorem 1 for LDS is now completely analogous to Sec. 3.5.

3.7. Proof of Theorem 2

The steps required to verify Theorem 2 are quite similar to the ones taken in the course of proving Theorem 1. Again we first ensure that the local (that is, uncoupled) dynamics is trivial. This is most conveniently done by relating $Q = Q_{a,b,c}$ to the standard logistic map [Katok & Hasselblatt, 1995].

Proposition 4. *Let R denote the quadratic map $R : x \mapsto \alpha x^2 + \beta x + \gamma$ with $\alpha, \beta, \gamma \in \mathbb{R}$ and $\alpha \neq 0$. If $(\beta - 1)^2 \geq 4\alpha\gamma$ then R is topologically conjugate to $F_\mu : x \mapsto \mu x(1 - x)$ with*

$$\mu = \mu(R) = 1 + \sqrt{(\beta - 1)^2 - 4\alpha\gamma}.$$

It is well-known (and easy to prove) that for $\mu > 2 + \sqrt{5}$ the logistic map F_μ has trivial dynamics in the sense that $\lim_{n \rightarrow \infty} |F_\mu^n(x_0)| = \infty$ for every $x_0 \in \mathbb{R} \setminus C$ where C is a Cantor set of Lebesgue measure zero; moreover $|F'_\mu(x)| > 1$ for all $x \in C$ in this case [Kraft, 1999; Zeller & Thaler, 2001]. In view of Proposition 4, for the map Q the condition $\mu(Q) > 2 + \sqrt{5}$ boils down to $c(8b + c - 6) > 5 + 2\sqrt{5}$, which in turn yields the lower bound

$$c > 3 - 4b + \sqrt{16b^2 - 24b + 14 + 2\sqrt{5}}. \tag{52}$$

On the other hand, we must have $b + (c/8) < 1$, i.e.

$$c < 8(1 - b). \tag{53}$$

Conditions (52) and (53) are consistent provided that $b < (11 - 2\sqrt{5})/16 \approx 0.4080$. Therefore, if Q is convex on $[0, 1/2]$ and

$$\begin{aligned} 0 < a < b < \frac{11 - 2\sqrt{5}}{16} \text{ as well as} \\ 3 - 4b + \sqrt{16b^2 - 24b + 14 + 2\sqrt{5}} \\ < c < 8(1 - b), \end{aligned} \tag{54}$$

then the local dynamics of Q is trivial: for a.e. $x_0 \in [0, 1]$ we have $\lim_{n \rightarrow \infty} Q^n(x_0) = x^*$ (see Fig. 1).

In the presence of nonzero spatial interaction we require that $x_j^n \in [0, 1/2]$ for all j with $1 \leq \|j - i^*\| \leq 2$ and all $n \in \mathbb{N}_0$. This can be ensured by assuming that $(1 - \varepsilon)b + \varepsilon < 1/2$ or equivalently

$$\varepsilon < \frac{1 - 2b}{2 - 2b} =: \hat{\varepsilon}_0. \tag{55}$$

To make the argument concerning the dynamics at site i^* as transparent as possible we will for the time being assume that $a = b$ even though, strictly speaking, this is impossible as Q was assumed to be C^1 ; we shall correct this ‘‘error’’ later. Under this assumption we have at site i^*

$$x_{i^*}^{n+1} = (1 - \varepsilon)Q(x_{i^*}^n) + \varepsilon b =: Q_\varepsilon(x_{i^*}^n).$$

Note that when restricted to $[1/2, 1]$ the family $(Q_\varepsilon)_{\varepsilon \geq 0}$ is a *full* family. Informally, this means that upon variation of ε the maps Q_ε will exhibit every dynamical behavior possible for a one-dimensional unimodal map (see [Katok & Hasselblatt, 1995] for details). In view of the statement of Theorem 2 we are only interested in periodic orbits here. As is well-known, for $0 < \mu \leq 2$ the map F_μ does not have any periodic orbit with primitive period $p > 1$. For the nontrivial morphogenesis of Q_ε to occur within the parameter range specified by (55) we require that $\mu(Q_\varepsilon) > 2$ for all $\varepsilon < \hat{\varepsilon}_0$. Since $\varepsilon \mapsto \mu(Q_\varepsilon)$ is decreasing this leads to $\mu(Q_{\hat{\varepsilon}_0}) > 2$ or equivalently

$$c > 4(1 - b)(3 - 4b). \tag{56}$$

For (56) to be consistent with the upper bound on c in (54) we must have $b > 1/4$. Furthermore, for simplicity we demand that (56) implies the lower bound on c in (54), which is the case provided that $b < (3/4) - 1 + \sqrt{21 + 8\sqrt{5}}/8 \approx 0.2748$. We there-

fore narrow down (54) by assuming that

$$\frac{1}{4} < b < \frac{3}{4} - \frac{1 + \sqrt{21 + 8\sqrt{5}}}{8} \quad \text{and} \\ 4(1 - b)(3 - 4b)c < 8(1 - b). \quad (57)$$

If parameters are chosen according to (57) then not only is the local dynamics of Q trivial but also Q_ε can have nontrivial periodic points only if $\varepsilon < \hat{\varepsilon}_0$. It follows from the properties of the quadratic family that for any $p \in \mathbb{N}$ there exists $\varepsilon_{(p)}$ such that $Q_{\varepsilon_{(p)}}$ has a super-attracting orbit $\{t_1, \dots, t_p\}$ of primitive period p . (All other periodic orbits which $Q_{\varepsilon_{(p)}}$ may have are unstable.) Consequently, there exist positive numbers $\kappa_1, \dots, \kappa_p$ with the property that the intervals $I_l := [t_l - \kappa_l, t_l + \kappa_l]$ are disjoint and, for all $l = 1, \dots, p$,

$$Q_{\varepsilon_{(p)}}(I_l) \subset I_{l+1} \quad \text{as well as} \\ m^1(Q_\varepsilon(I_l)) \leq \frac{1}{2}\kappa_{l+1} = \frac{1}{4}m^1(I_{l+1}); \quad (58)$$

here an index $p + 1$ is understood to equal 1. Note that the second property in (58) implies that $I_{l+1} \setminus Q_{\varepsilon_{(p)}}(I_l)$ consists of two intervals each of which is at least $(1/2)\kappa_{l+1}$ long.

We now drop the hypothetical assumption $a = b$, and we fix $T \in \mathcal{M}^1$ with $\|T - Q\|_{\text{Lip}} < \delta$ as the local map for a CML. Assuming that $x_j^n \in [0, 1/2]$ for $1 \leq \|j - i^*\| \leq 2$ we have the immediate estimate

$$|x_{i^*}^{n+1} - Q_{\varepsilon_{(p)}}(x_{i^*}^n)| \leq |\varepsilon - \varepsilon_{(p)}| + \delta + \varepsilon(b - a). \quad (59)$$

Let $\kappa := \min_{l=1}^p \kappa_l$. Since we want the right-hand side of (59) to be less than $(1/2)\kappa$, we require that

$$b - a < \frac{\kappa}{2\hat{\varepsilon}_0} = \kappa \frac{1 - b}{3 - 6b}. \quad (60)$$

Furthermore, we define the threshold values

$$\varepsilon_2 := \varepsilon_{(p)} - \frac{1}{6}\kappa, \quad \varepsilon_3 := \min \left\{ \varepsilon_{(p)} + \frac{1}{6}\kappa, \hat{\varepsilon}_0 \right\}, \quad (61)$$

which obviously satisfy $\varepsilon_2 < \varepsilon_{(p)} < \varepsilon_3 < \hat{\varepsilon}_0$. To justify the assumption that $x_j^n \in [0, 1/2]$ for all $j \neq i^*$ in the cluster and all $n \in \mathbb{N}$ we demand that $(1 - \varepsilon)b + \varepsilon + \delta < 1/2$ for all $\varepsilon < \varepsilon_3$, which leads to

$$\delta < (1 - b)(\hat{\varepsilon}_0 - \varepsilon_3) =: \hat{\delta}_1.$$

Also, the local dynamics of T will be trivial provided that $\delta < \hat{\delta}_2$ with a sufficiently small $\hat{\delta}_2$. (An explicit formula for $\hat{\delta}_2$ can easily be worked out from e.g. [Zeller & Thaler, 2001].) Moreover, triviality of local

dynamics will persist for sufficiently small perturbations. This intuitively obvious statement can be justified as follows. Let $Q_\varepsilon^\pm(x) := (1 - \varepsilon)Q(x) + \varepsilon((b + a)/2) \pm \varepsilon((b - a)/2)$ and define points x_ε^\pm and y_ε^\pm as in the case of piecewise linear maps (cf. Fig. 3), that is, $1/2 < Q_\varepsilon^\pm(x_\varepsilon^\pm) = x_\varepsilon^\pm < 3/4$ and $Q_\varepsilon^\pm(y_\varepsilon^\pm) = x_\varepsilon^\pm$, $y_\varepsilon^\pm > 3/4$. Furthermore there exist points p_ε^\pm , q_ε^\pm such that $x_\varepsilon^\pm < p_\varepsilon^\pm < 3/4 < q_\varepsilon^\pm < y_\varepsilon^\pm$ and $Q_\varepsilon^\pm(p_\varepsilon^\pm) = Q_\varepsilon^\pm(q_\varepsilon^\pm) = y_\varepsilon^\pm$. Define now an increasing family of sets $J(\varepsilon) := \bigcup_{0 \leq \gamma \leq \varepsilon} [x_\gamma^+, p_\gamma^-] \cup [q_\gamma^-, y_\gamma^+]$. Clearly,

$$f(\varepsilon) := \min_{t \in J(\varepsilon)} |(Q_\varepsilon^\pm)'(t)| = (1 - \varepsilon) \min_{t \in J(\varepsilon)} |Q'(t)|$$

defines a continuous, decreasing function with $f(0) > 1$. Thus there exists $\varepsilon_1 > 0$ such that $f(\varepsilon_1) > 1$. As for piecewise linear maps (Fig. 3) repeat the above argument with Q replaced by an arbitrary T with $\|T - Q\|_{\text{Lip}} < \delta$; in particular, define $\tilde{J}(\varepsilon) := \bigcup_{0 \leq \gamma \leq \varepsilon} [\tilde{x}_\gamma^+, \tilde{p}_\gamma^-] \cup [\tilde{q}_\gamma^-, \tilde{y}_\gamma^+]$ with the corresponding points $\tilde{x}_\varepsilon^\pm$, $\tilde{y}_\varepsilon^\pm$, $\tilde{p}_\varepsilon^\pm$, $\tilde{q}_\varepsilon^\pm$. The function $\tilde{f}(\varepsilon) := \min_{t \in \tilde{J}(\varepsilon)} |(T_\varepsilon^\pm)'(t)|$ continuously depends on both ε and δ , and $\tilde{f}(\varepsilon) \geq (1 - \varepsilon)(\min_{t \in \tilde{J}(\varepsilon)} |Q'(t)| - \delta)$ as well as $\tilde{f} = f$ for $\delta = 0$. Pick $\hat{\delta}_3 > 0$ such that $\tilde{f}(\varepsilon) > 1$ for all $\varepsilon < \varepsilon_1$ and $\delta < \hat{\delta}_3$. Finally, in view of (59) we set $\hat{\delta}_4 := (1/6)\kappa$ and $\hat{\delta} := \min_{k=1}^4 \hat{\delta}_k$.

We are now in a position to summarize our findings as follows. Let parameters a, b, c of the local map $Q_{a,b,c}$ be chosen according to (57) and (60) and assume that $\|T - Q\|_{\text{Lip}} < \hat{\delta}$. Then for $\varepsilon < \varepsilon_1$ the dynamics at all sites in the cluster is regular; in particular, we will observe that $x_{i^*}^n$ is eventually in $[0, 1/2]$ for a.e. $x_{i^*}^0$. If on the other hand $\varepsilon_2 < \varepsilon < \varepsilon_3$ then $(x_{i^*}^n)_{n \in \mathbb{N}}$ visits a periodic sequence of intervals I_l , hence oscillates in a pseudo-periodic manner, whereas all other sites in the cluster perform a regular motion in the left half of the interval. This scenario takes place whenever $x_j^0 \in [0, 1/2]$ for all $1 \leq \|j - i^*\| \leq 2$ and $x_{i^*}^0 \in \bigcup_{l=1}^p I_l$. The completion of the proof of Theorem 2 is now identical with the corresponding part in the proof of Theorem 1.

We conclude this section with a numerical example and a remark. We fix $p = 3$ as the period for which we wish to find an appropriate coupling intensity. It is well-known that F_μ has a super-attracting 3-periodic orbit for $\mu = \mu_3$ with

$$\mu_3 = 1 + \frac{1}{\sqrt{3}} \\ \times \sqrt{11 + 2\sqrt[3]{100 - 12\sqrt{69}} + 2\sqrt[3]{100 + 12\sqrt{69}}} \\ \approx 3.8319;$$

correspondingly, a possible (yet very pessimistic) value for κ would be $\kappa = 2^{-15}3^{-2} \approx 3.3 \cdot 10^{-6}$. Choosing parameters according to (57) and (60) as

$$b = 0.26, \quad c = 5.9, \quad a > b - \frac{1}{2}\kappa,$$

yields $\hat{\varepsilon}_0 = 0.3243$ and, via the equality $\mu(Q_{\varepsilon(3)}) = \mu_3$,

$$\varepsilon_{(3)} = 0.1092. \quad (62)$$

For a small interval around $\varepsilon_{(3)}$ a stable, regular pseudo-3-periodic motion will therefore be observed at sites i^* , whereas the surrounding sites in the cluster perform a stable oscillation in the left half of the interval $[0, 1]$. On the other hand, for small ε all sites in the cluster will eventually settle down near the fixed point x^* of the unperturbed map. For this concrete example, the reader might be struck by the tiny size of κ . It may, however, be worth recalling that for the autonomous map $Q_{\varepsilon(p)}$, i.e. for the (hypothetical) case $a = b$, the domain of attraction of the super-attracting p -periodic orbit is much larger than $\bigcup_{l=1}^p I_l$: except for a Cantor set of measure zero *all* points in $[x_\varepsilon^+, y_\varepsilon^+]$ will in fact be attracted by the stable orbit [Katok & Hasselblatt, 1995]. Numerical evidence indicates clearly that also in the nonautonomous case $a < b$ the domain of attraction for the pseudo- p -periodic motion in question will typically be *much* larger than $\bigcup_{l=1}^p I_l$.

4. Concluding Remarks

The results presented in this article can be generalized in a number of ways. Obviously, the requirement that all local maps are identical can be dropped; our results will hold *mutatis mutandis* as long as the local maps are close to each other (and to an appropriate model map) in the corresponding topology. Also, other types of diffusive coupling can be considered. For example, it is straightforward to adapt the arguments of the present paper to the class of couplings considered in [Afraimovich & Fernandez, 2000] as in some sense the most general type of diffusive coupling. It is worth noting though that the required size of the cluster may vary, depending on the actual structure of the coupling under consideration. Finally, similar results can be formulated and proved quite easily for multimodal local maps. All this clearly indicates that the peak-crossing bifurcation can be observed in a large variety of spatially extended dynamical systems. We think, however, that the results presented already

give a clear picture of the robustness and generality of this mechanism and we will therefore not pursue any of these potential generalizations here.

As has been demonstrated in this article, peak-crossing leads to the appearance of some (in fact infinitely many) individual sites which oscillate chaotically and which are isolated from each other by (at least) clusters of regular behavior. While being intrinsically a consequence of spatial interactions, the peak-crossing bifurcation may therefore be just a transitional step on the route to more global chaos. Observe for instance that the thresholds for ε for this bifurcation to occur, as computed on the basis of our analysis (see e.g. (42) and (62)), are overall rather small (albeit still distinctively nonzero). One may expect that with further increasing ε other, more complicated bifurcations should occur by means of which the isolated chaotic sites created via peak-crossing could start to communicate and thus eventually produce collective (spatially) chaotic modes. The detection and analysis of bifurcations of this type constitutes a most important issue in the development of the theory of space-time dynamics.

Acknowledgment

While being a visitor at Georgia Tech the first author was supported by a MAX KADE research fellowship.

References

- Afraimovich, A. & Fernandez, B. [2000] "Topological properties of linearly coupled expanding map lattices," *Nonlinearity* **13**, 973–993.
- Aubry, S. [1997] "Breathers in nonlinear lattices: Existence, linear stability and quantization," *Physica* **D103**, 201–250.
- Bunimovich, L. A. & Sinai, Y. G. [1988] "Space-time chaos in coupled map lattices," *Nonlinearity* **1**, 491–516.
- Bunimovich, L. A. [1995] "Coupled map lattices: One step forward and two steps back," *Physica* **D86**, 248–255.
- Bunimovich, L. A. & Venkatagiri, S. [1996] "Onset of chaos in coupled map lattices via the peak-crossing bifurcation," *Nonlinearity* **9**, 1281–1298.
- Bunimovich, L. A. & Venkatagiri, S. [1997] "On one mechanism of transition to chaos in lattice dynamical systems," *Phys. Rep.* **290**, 81–100.
- Chaté, H. & Courbage, M. [1997] "Special issue: Lattice dynamics," *Physica* **D103**, 1–611.

- Kaneko, K. [1993] *Theory and Applications of Coupled Map Lattices. Nonlinear Science: Theory and Applications* (John Wiley, Chichester).
- Katok, A. & Hasselblatt, B. [1995] *Introduction to the Modern Theory of Dynamical Systems* (CUP, Cambridge).
- Kraft, R. L. [1999] "Chaos, cantor sets, and hyperbolicity for the logistic maps," *Amer. Math. Monthly* **106**, 400–408.
- MacKay, R. S. & Aubry, S. [1994] "Proof of existence of breathers for time-reversible or Hamiltonian networks of weakly coupled oscillators," *Nonlinearity* **7**, 1623–1643.
- Zeller, S. & Thaler, M. [2001] "Almost sure escape from the unit interval under the logistic map," *Amer. Math. Monthly* **108**, 155–158.